# Modeling Methane Migration and Oxidation in Landfill Cover Materials with TOUGH2-LGM

David Rannaud[1], Alexandre Cabral[2,*], and Suzanne E. Allaire[3]

*1 Tecsult Inc., Montreal, Quebec, Canada (former graduate student, Université de Sherbrooke)*

*2 Department of Civil Eng., Université de Sherbrooke, Quebec, Canada J1K 2R1*

*3 Department of Soils and Agro-environmental Engineering, Université Laval, Quebec, Canada, G1K 7P4*

** Corresponding author*

## Abstract

Methane oxidation within a Passive Methane Oxidation Barrier (PMOB) and the downward migration of molecular $O_2$, whose presence is necessary for the oxidation reaction to occur, were simulated using the finite element simulator TOUGH2-LGM. The goals of the study were to validate the use of TOUGH2-LGM by reproducing real field profiles obtained under different conditions and to evaluate the depth of $O_2$ penetration under several conditions. TOUGH2-LGM handles both advective and diffusive gas fluxes. The oxidation reaction was simulated by imposing a Neumann condition, i.e. $CH_4$ was extracted from pre-determined elements. The main variables of concern were the degree of water saturation of the PMOB, the pressure differential between its base and the surface, the position and thickness of the oxidation front and, finally, the oxidation rate, i.e. the rate at which $CH_4$ was removed from the system. Other important variables, such as the gas permeability and diffusion coefficient were obtained in the laboratory. Inspection of the results shows that TOUGH2-LGM was able to quite accurately reproduce the field profiles. The simulator also makes it possible to predict the depth of $O_2$ penetration as a function of pressure differential and humidity within the PMOB. This type of information is fundamental for the design of effective biocovers.

***Keywords:*** ***methane oxidation, biocovers, landfill gas, oxidation efficiency, gas profiles, TOUGH2-LGM***

Rannaud, D., Cabral, A.R. and Allaire, S. E.# (2009). "Modeling methane migration and oxidation in landfill cover materials with TOUGH2-LGM." Water, Air, and Soil Pollution 198(1-4): 253-267

# Introduction

Methane ($CH_4$) is a potent greenhouse gas with an impact 25 times higher than that of $CO_2$, based on a 100 years observation period (IPCC 2007). Its atmospheric concentration is increasing at a rate of 0.6% per year and nearly 70% of this increase is related to human activities, with landfills contributing to nearly 17% of this amount (IPCC 2001).

Landfill $CH_4$ emissions can be reduced by bacterial oxidation (methanotrophic activity) during its migration in landfill cover materials, which could be optimized through proper management and selection of the properties of the cover material (Humer and Lechner 2001a; Gebert and Gröngröft 2006a). Oxidation of $CH_4$ into $CO_2$ depends on gas and liquid migration across the cover, meteorological conditions (such as temperature and barometric pressure), physico-chemical properties of the cover material influencing gas movement, nutrient availability to bacteria (mainly N and P according to Hilger and Humer 2003), and sufficient quantities of $CH_4$ and $O_2$. According to De Visscher et al. (1999), for efficient microbial oxidation of $CH_4$, the $O_2$ concentration must be higher than 3%, while for Gebert et al. (2003) 2% of $CH_4$ is sufficient, although Gebert et al.'s experiments showed that full activity did not develop until the concentration reached approximately 8%. However, these kinds of "limiting concentrations" must be considered with care; indeed, the $O_2$ concentration at a certain depth within a profile can be lower than 3%, while the $N_2$ concentration may be equal to or greater than 11.4% (3% divided by the normal $[O_2\%]/[N_2\%]$ ratio in air, i.e. 0.264). This situation has been observed for several series of field data obtained by the authors (not presented here). In these cases, it can be hypothesized that $O_2$ is being consumed by microorganisms as it becomes available.

The relative importance of each of the above-mentioned parameters on the efficiency of $CH_4$ oxidation is not yet well understood. The large number of parameters combined with the variability in weather and cover material properties render the problem complex. It isn't always feasible to evaluate a large range of conditions in laboratory and field environments in order to optimize oxidation. The use of numerical modelling thus constitutes an important designing tool, if properly used and supported (calibrated) by laboratory and field testing.

Among available simulators that can handle convective and diffusive fluxes of gases through porous media, THOUGH2-LGM (Transport of Unsaturated Groundwater and Heat - Landfill Gas Migration) was specifically developed to handle the conditions found in landfill covers (Nastev 1998). THOUGH2-LGM was successfully utilized in problems pertaining to production and collection of biogas, as well as gas migration through unsaturated porous or fractured media (Bour et al. ; Nastev et al. 2003; Vigneault et al. 2004).

The goal of this study was to develop a numerical approach to simulate $CH_4$ and $O_2$ migration as well as $CH_4$ oxidation in landfill cover material using TOUGH2-LGM, validate model simulations against field data, and study the relative importance of advection and diffusion on the depth of $CH_4$ oxidation (and $O_2$ penetration) in cover materials.

# Background

## Gas migration

Advection, diffusion and biological or chemical reactions influence most gas migration in unsaturated porous media. This paper considers only gas transport processes in the soil gas phase. Advection refers to gas movement due to a total pressure gradient. It can be calculated using equation 1 (Bear and Bachmat 1991):

$$J_a = -\frac{\rho \times K_g}{\eta}\frac{\partial P}{\partial z} \qquad [1]$$

where $J_a$ is the advective gas flux (g $m^{-2}$ $s^{-1}$), $K_g$ is the gas permeability ($m^2$), $\rho$ is the gas density (g $m^{-3}$), $\eta$ is the gas dynamic viscosity (Pa s), $P$ is the total pressure in the soil gas phase (Pa), $z$ is the distance (m) of measurement of flux. $K_g$ can be calculated from equation 2:

$$K_g = K_{re\,lg} \times K \qquad [2]$$

where $K_{relg}$ is the relative gas permeability (adim.) and $K$ is the intrinsic permeability ($m^2$). Theoretically, $K_{relg}$ can have a value ranging from 0.0 in saturated soils to 1.0 in completely dry conditions. $K_{relg}$ can be calculated with one of several relationships available in the literature (Allaire et al. 2007). For the present study, Corey's model (1957) – equation 3 - was used:

$$K_{re\,lg} = (1 - S_{we})^{n^*} \qquad [3]$$

where $n^*$ is an empirical parameter often equal to 2 and $S_{we}$ is the normalized degree of water saturation of the media ($m^3$ $m^{-3}$), given by equation 4:

$$S_{we} = \frac{S_w - S_{wr}}{1 - S_{gr} - S_{wr}} \qquad [4]$$

where $S_w$ is the water-filled porosity saturation ($m^3$ $m^{-3}$), $S_{wr}$ is the water-filled porosity saturation at the residual water content ($m^3$ $m^{-3}$), and $S_{gr}$ is the air-filled porosity saturation at water saturation ($m^3$ $m^{-3}$).

Gas diffusion refers to gas movement associated with a gradient in partial pressure i.e. in gas concentration. In this study, only molecular diffusion is considered. Diffusive gas fluxes can be calculated using Fick's first law, which, for a one dimensional permanent flux, takes the form of equation 5:

$$J_d = -D_s \frac{\partial C}{\partial z} \qquad [5]$$

where $J_d$ is the diffusive gas flux (g $m^{-2}$ $s^{-1}$), $D_s$ is the soil gas diffusion coefficient ($m^2$ $s^{-1}$), and $C$ is the gas concentration (g $m^{-3}$). $D_s$ varies with gas and porous media properties. The property of the porous media most influencing gas movement is the air content ($\theta_a$; $m^3_{air}$ $m^{-3}_{sol}$), which depends on the volumetric water content ($\theta_w = \theta_T - \theta_a$; $m^3_{water}$ $m^{-3}_{soil}$, where $\theta_T$ is the soil total porosity; $m^3_{porosity} m^{-3}_{soil}$). Laboratory experiments were conducted to measure *Ds* and evaluate the most performing model for the porous media used in this study. Among a series of models available in the literature, (Moldrup et al. 1997) – equation 6 - was used to calculate *Ds*:

$$\frac{D_s}{D_o} = 0{,}66\theta_a\left(\frac{\theta_a}{\theta_T}\right)^{\frac{12-m}{3}} \quad [6]$$

where $D_o$ is the diffusion coefficient of the gas in the air ($m^2\ s^{-1}$) and $m$ is an empirical parameter. Values suggested for $m$ range from 3, for intact soils, to 6, for repacked soils (Moldrup et al. 1997).

## Methane oxidation

$CH_4$ can be oxidized into $CO_2$ by means of chemical or biological reactions. Only biological oxidation is considered in this paper, because it is the most important process affecting $CH_4$ concentration in landfill cover materials (Kallistova et al. 2005). $CH_4$ oxidation can be described in its simplified form by reaction 1 (Kjeldsen 1996):

$$CH_4 + 2\ O_2 \rightarrow CO_2 + 2\ H_2O + \text{heat};\ \Delta G° = -780\text{kJ/mol}\ CH_4 \qquad [R1]$$

If no oxidation occurs and assuming that both $O_2$ and $N_2$ migrate at the same rate within the soil profile (which is valid under steady state conditions), the $[O_2\%]/[N_2\%]$ ratio typically found in the lower atmosphere would remain constant at about 0.264 (20.9%/79.1%). Ratios lower than that of the air would then indicate consumption of $O_2$. The lower the decomposable organic matter content of the cover material, the lower the consumption of $O_2$ for soil respiration and the greater the amount of $O_2$ used for $CH_4$ oxidation. For the purposes of this paper, $O_2$ consumption is considered to result solely from oxidation of $CH_4$.

## Passive methane oxidation barriers (PMOB)

PMOBs are covers constituted usually (but not solely) of a coarse gas distribution layer and a substrate layer. They can be designed to operate either as biocovers or biofilters. Biofilters cover a small area, whereas biocovers are meant to cover wide areas (eventually the entire footprint of a landfill cell), thereby being constructed following the same gentle and steep slopes normally found in landfills.

Several types of PMOB designs have been proposed: in some cases, additional layers to the cover system have been proposed in order to be able to count on passive oxidation (e.g. Ameis site, in Austria; Huber-Humer and Lechner 2002). In Germany, Gebert and Gröngröft (2006a) proposed a biofilter consisting mainly of crushed porous clay covered with a thin layer of top soil. In France, Morcet et al. (2003) reported experiments conducted at the Montreuil-sur-Barse site, where a PMOB was built consisting of 0.30 m of organic soil on top of a GCL (geotextile clay liner), placed on top of a layer of sand. Four PMOBs have been built in Australia with a profile of 1.2 m of organic soil (different for each of the four) on top of 0.5 m of gravel (Dever et al. 2005). As can be observed, there are a multitude of possible PMOB designs. There is also great variation in the oxidation efficiencies obtained (e.g. 10% reported by Czepiel et al. (1996), 70% recorded by Hettiaratchi and Pokhrel (2003), etc.).

Many factors influence PMOB performance (thus oxidation efficiency), such as water infiltration, changes in atmospheric pressure, and soil temperature. Infiltration of water into sloping biocovers can affect its capacity to oxidize $CH_4$ due to unsaturated water flow along the interface between the substrate and the gas distribution layer caused by the development of a

hydraulic break at this interface (Berger et al. 2005; Cabral et al. 2007a). This hydraulic break, which is caused by differences in hydraulic properties of the two layers, can lead to an accumulation of infiltrating water at and above the interface, thereby causing an increase of $S_w$ and a decrease in $\theta a$, which in turn affect gas fluxes (Boeckx and Van Cleemput 2000; Humer and Lechner 2001b). It has been suggested that gas flux becomes very low when the water-filled porosity saturation, $S_w$, is in the vicinity of 85%, which is approximately the point beyond which there is air occlusion (Aachib et al. 2004; Nagaraj et al. 2006). This results in low $O_2$ diffusion, which may cause a significant decrease in microbial oxidation.

Changes in barometric pressure (more precisely, the differential pressure between the waste mass and the atmosphere) directly influence $O_2$ flux from the surface to the depth, thus $O_2$ availability, thus PMOB performance. This impact increases as the air-filled porosity of the PMOB increases (Galle et al. 2001; Gebert and Gröngröft 2006b). Soil temperature influences biological activity, biochemical reactions and gas flux. Methanotrophic bacteria activity is very low below 5°C, increases with increasing temperature (Czepiel et al. 1996; Boeckx et al. 1999) and seems optimal around 30 °C (Nolting et al. 1995). Zeiss (2006) used a passive heat exchange system to transfer heat from inside the landfill to a compost biofilter bed integrated into the cover of a municipal solid waste landfill in Western Canada. The heat exchange raised the filter temperature to 14-18 °C even during the cold winter months, which, according to the authors, resulted in an increased performance of the biofilter. Since temperature affects gas concentration and pressure, an increase in temperature results in faster gas movement.

# Materials and Methods

## Description of the experimental field plots

Three POMB (2.75 m wide x 9.75 m long) cells were constructed on an existing landfill site (St-Nicéphore, Quebec, Canada). This section of the cover followed a 3% slope (direction of the main axis of the PMOBs). The characteristics and tests pertaining to only two of them (PMOB1 and PMOB2) are presented and discussed herein. The general concept consists of a coarse layer covered by a substrate layer. Polystyrene foam panels (0.15-m thick) surround each PMOB to provide thermal insulation from the exterior, which limits water migration due to thermal gradients within the substrate. A schematic representation of PMOB1 is presented in Figure 1. PMOB2 was built in the existing cover and isolated from it by a geomembrane and the polystyrene foam panels. The base of PMOB1 sits directly on the 3.5-year old waste mass (Figure 1). Consequently, the biogas flux was not controlled. For PMOB2, biogas was provided by means of a feed system (5-cm external $\phi$ ADS tubes) connected to a dedicated biogas well. An insertion mass flow meter (model SIG0515DC24DIGRG2, from Aysix-Sage), connected to a datalogger (SP-4000-4CW, from Veritek) made it possible to monitor the influx of biogas in PMOB2.

The role of the coarse material layer is to uniformly distribute the biogas at the base of the substrate, whereas the role of the nutrient-rich substrate is to favour microbial oxidation of $CH_4$. The coarse layer is composed of two sub-layers: the top-most sub-layer, a transitional layer, is 0.1 m thick and is composed of net gravel ($\phi$ = 6.4 mm), whereas the bottom-most sub-layer is composed of uniform coarse gravel (grain-size diameter ($\phi$) = 12.7 mm).

The 0.8-thick substrate layer is composed of a sand:compost (1:5 v/v) mixture with 17.8% organic matter content on a dry mass basis ($g_{volatile\ matter}/g_{dry\ soil}$). The 2-year-old compost was provided by a local producer that composted a mix of municipal sewage sludge and sludge from pulp and paper and agri-food industries. Respirometry tests were performed by an external certified laboratory on duplicate samples of the mixture, following the BNQ 0413-200/2005-art 9.3.1 standard (BNQ 2005). The results obtained (268 and 230 mg of $O_2$ consumed per hour per kg of volatile solids on a dry matter basis) indicate that, according to this standard, the material can be considered mature, because its respirometry values are lower than 400 $mgO_2/kg_{v.s}\,h^{-1}$. The substrate material was sieved with a 12-mm industrial sieve and then compacted in 0.2-m thick layers using a vibrating plate to obtain a dry density of 840 $kg/m^3$, which corresponds to 85% of the maximum Standard Proctor.

Aluminum gas sampling tubes equipped with a septum at the top were installed at four equally distributed downgradient points along the main axis of each cell. At each point, the tubes were installed at 6 depths (Fig. 1b). On a weekly basis, vertical concentration profiles of $CO_2$, $CH_4$ and $O_2$ in the pore voids of the PMOB were manually determined. First, one equivalent volume of gas contained in each aluminum tube was flushed using a simple 50-ml syringe. One hour after flushing, gas samples were taken and the concentrations of the 3 gases were determined using a Portable Gas Meter (Columbus Instruments Inc.). This delay was found to be sufficient to re-equilibrate the pore gas composition. Between each sampling, a syringe of ultra zero gas was injected into the gas meter to purge it.

At these same points on the cells, probes for measurement of water content ($\theta$), temperature and gas concentration were installed at four equally distributed downgradient points along the main axis of each cell. Four capacitance probes for measuring the soil water content ($ECH_2O$ EC-5, from Decagon Inc.) were installed at evenly distributed depths along each profile, while temperature probes (HOBO U12 Outdoor, from ONSET Inc.) were installed at four depths in each cell (Fig. 1b) - though not evenly distributed, because a greater concentration of temperature data near the surface was desired. The temperature and water content probes were connected to dataloggers. Meteorological data, including precipitation, air temperature and barometric pressure, were recorded every 30 minutes by a weather station (Vantage Pro 2, from Davis Instruments) installed near the experimental plot.

## Physical parameters

**Ds and Kg:** The diffusion coefficient, $D_s$, was determined using the "small-open" method described in Allaire et al. (2007) over a wide range of degrees of water saturation. Intact soil cores were sampled directly on site in the substrate layer. Moldrup et al.'s (1997) (Equ. 6) model using m=6 performed best among different models available in the literature.

The gas permeability, $K_g$, of the substrate was determined for several degrees of saturation ($S_w$) using a home-made soap film flow meter and following a method very similar to the one presented by Maciel et Jucá (2000). The model that best fitted the results was the Corey (1957) model (equ. 3) with $K = 5.5x10^{-13}$ $m^2$, n*=1, $S_{wr}$=44 %, et $S_{gr}$=0 %.

**Pressure differential between the waste mass and the atmosphere:** Before pressure transmitters were installed, which occurred only recently, in 2007, advective flux was estimated from data obtained using a mass flow meter that recorded the influx into PMOB2. Recent pressure transmitter data indicate that the pressure differentials between the bottom of the PMOBs and the atmosphere varied between -0.3 kPa and 0.3 kPa. Most of the time, the values were less than 0.08 kPa, which is in the range used in the simulations presented below.

## The TOUGH2-LGM Simulator

TOUGH2-LGM (Nastev 1998) uses an integral finite difference numerical schematic representation solved with the Newton-Raphson iteration approach. It makes it possible to model the transport of atmospheric air (a mixture of 20.9% of $O_2$ and 79.1 % of $N_2$), water, carbon dioxide ($CO_2$) and methane ($CH_4$) in the liquid and gas phases, by advection and diffusion. TOUGH2-LGM can also calculate heat fluxes and gas production by the waste mass as a function of waste mass age. It can solve Dirichlet or Neumann boundary conditions for gas flux (Nastev 1998). In the case of a Dirichlet boundary condition, conditions must be specified for concentration, pressure, temperature, etc. This is the type of condition applied in the model presented below. In the case of a Neumann boundary condition, a mass flux or heat flux condition must be specified. This is the type of condition imposed to simulate the oxidation phenomenon, as described below.

Even though the simulator allows for water and gas migration analysis, it can simulate transport in only one phase. In the present study, flux was investigated in the gas phase only. This is convenient (thus adopted here) because the modeller can be freed from the necessity of providing further water retention and hydraulic conductivity data. However, the model requires a value for $K_g$ and this parameter varies as a function of $S_w$, which is also provided by the modeller. Once $S_w$ is given, $K_g$ is obtained from equations 2, 3 and 4, using the parameters adjusted based on the gas permeability data previously presented.

TOUGH2-LGM uses either the Millington and Quirk (1961) or the Lai (1976) model to calculate $D_s$ based on $S_w$. Since the Moldrup et al. (1997) model for the estimation of $D_s$ from $S_w$ performed better for the substrate of this study, $D_s$ values were first calculated using Moldrup et al. (1997). Fictive values of the parameters in the Lai (1976) model were then input so that the same $D_s$ predicted with Moldrup et al. (1997) were eventually obtained by TOUGH2-LGM.

Since TOUGH2-LGM can not handle the oxidation process, a Neumann condition was imposed to simulate the oxidation of $CH_4$ into $CO_2$ within the substrate. This means that $CH_4$ was extracted from the elements where oxidation occurs. The position of these elements (i.e. the position of the oxidation front) and the rate of extraction of $CH_4$ from the system (actually, the volume of $CH_4$ extracted over time) are two other variables that needed to be adjusted during the simulations. With the rate of extraction and the $CH_4$ flow entering the system, it is possible to calculate the "simulation oxidation efficiency".

TOUGH2-LGM does not reproduce a real oxidation reaction, i.e. actual $O_2$ consumption and the consequent $CO_2$ production; as a consequence, in order to simplify the problem, the simulations with consideration of oxidation concentrated on the migration and extraction of $CH_4$ only. The fact that $CH_4$ is extracted from the model and that no gas replaces it leads to the creation of a

vacuum, which, in turn, results in the creation of a slight pressure differential. In fact, this is somewhat similar to what happens during oxidation (reaction 1), because three gas molecules (1 $CH_4 + 2O_2$) result in only one gas molecule ($CO_2$), which also creates a vacuum.

All parameters relative to water and heat flux, and $O_2$ and $CH_4$ concentrations at the soil surface were given as input data in the simulations. For the sand-compost mixture, the heat conductivity ($\lambda$) and the heat mass capacity (Cv), calculated according to Jury et al. (1991), are 1.69 W $m^{-1}$ $K^{-1}$ and 2041.2 J $kg^{-1}$ $K^{-1}$ respectively. The temperature of all the simulations presented is 20 °C, which is an average value of the substrate temperature in the field for the periods studied (data not presented). The temperature variations for the dates studied weren't considered great enough to significantly influence the density and diffusivity of the gases. Simulations were completed in 1D although TOUGH2-LGM can handle 2D and 3D. A schematic representation of a typical simulation is presented in Figure 2. The values of the input parameters are presented along with the presentation of the results.

# Results

## Model validation without $CH_4$ oxidation

Model validation was performed based on field data for October 2, 2006, when oxidation was almost absent, i.e. the profile was practically vertical, meaning that there was no abatement of $CH_4$ (see Figure 3). Gas concentrations of $CO_2$, $O_2$, and $CH_4$ at the lower boundaries and within the profile were obtained from gas probes in PMOB2 and the values in Figure 3 represent an average from the values obtained at the 4 sampling points (for each depth) along the main axis of the PMOB. At the top boundary, the concentrations of $CH_4$ and $CO_2$ were considered nil, whereas the $O_2$ concentration was set at 20.9%.

On Oct. 2nd, pressure transducers had not been installed yet at the bottom of PMOB2; as a consequence, the pressure differential ([redacted]) had to be estimated based on the recorded flux by the mass flow meter. The pressure differential was obtained by adjusting the simulated flux until it equalled the measured flux. For this date, the pressure differential was 0.14 kPa, a value considered high considering the above discussion concerning pressure differential.

$K_g$ was calculated based on water content data for this date (recorded by the data loggers connected to water content probes) and using equations 2, 3 and 4. On Oct. 2nd the degrees of saturation were 72% for the top and 77% for the bottom and the respective values of $K_g$ were 2.8 x $10^{-13}$ and 2.3 x $10^{-13}$ m². $D_s$ values were calculated using the same data and applying equation 6. For Oct. 2nd, the values of $D_s$ were 1.7 x $10^{-7}$ and 9.5 x $10^{-8}$ m²/s. The profiles obtained by simulation are very similar to those in the field, which shows that the TOUGH2-LGM model is able to quite accurately reproduce the gas profiles.

## Sensitivity to Ds and Kg

Model sensitivity was conducted on $D_s$, $K_g$, and the pressure gradient using the same Oct. 2nd values for these parameters. Sensitivity simulations were performed with values of $D_s$, 0.1 $D_s$, 0.5 $D_s$, and 2 $D_s$ and for two values of $\Delta P$: 0.14 and 0.02 kPa. Inspection of the results presented

in Figure 4 shows that $D_s$ is a parameter which greatly affects gas concentration profiles. In fact, a variation of $D_s$ by one order of magnitude results in a significant change in gas concentration profiles and even more so when ΔP is low (because the importance of diffusion becomes greater). The more $D_s$ increases, the faster $CH_4$ migrates towards the surface; one might thus expect to obtain a sharper (more vertical) profile, which is not the case in Figure 4. In fact, an increase in $D_s$ also means that more air enters the model, which dilutes the $CH_4$ concentration in the pores, leading to the profiles obtained.

The flux variations were in the order of 1% for all the values of $D_s$ when ΔP is 0.14kPa. For lower values of ΔP, such as 0.02 kPa, the diffusive flux becomes very large compared with the advective flux and the flux variations caused by the variations of $D_s$ are more in the order of 20% (also see the discussion about the data from Table 1).

For the October 2nd simulation (Figure 4a; where ΔP = 0.14 kPa), the sensitivity to $K_g$ is very high. The high value of ΔP implies a very large advective flux compared to the diffusive flux. In fact, the $K_g$ sensitivity studies for this simulation have shown that a 50% variation of the $K_g$ value implied a variation of approximately 50% of $CH_4$ outfluxes. However, for a series of simulations with a lower ΔP (0.02 kPa), the sensitivity of the results to $K_g$ decreased, while the sensitivity to Ds increased. Regardless, the model is sensitive to variations of $D_s$ and $K_g$, with magnitudes that depend on the predominant phenomenon (advection or diffusion), as discussed below. Therefore, accurate determination of $D_s$ as a function of $S_w$ is necessary. It may also be necessary to regularly adjust $D_s$ over time, as the cover material is submitted to settlement, changing the pore structure, thus $D_s$.

## Model validation considering $CH_4$ oxidation

The model was also validated for conditions under which oxidation occurred. Three groups of profiles obtained from PMOB1 were selected, corresponding to 3 different dates in 2006. For the first two (Aug. 15 – Figure 5 - and Aug. 8 - Figure 6), the decrease in $CH_4$ concentration was abrupt, whereas for Sep. 1st (Figure 7) this decrease was not as clear cut as for the other two. But in all cases an oxidation pattern was evident, i.e. there was a clear decrease in $CH_4$ concentrations.

**Aug 15, 2006:** This is the date when the most significant drop in $CH_4$ concentration for the year was obtained (Figure 5). The values of $S_w$ were 87% and 91% for the upper (surface to depth of 0.4 m) and lower (0.4 to 0.8 m) parts of the profile, respectively. The $CH_4$ concentration at the base of the PMOB was 52%. The pressure differential, ΔP, is the only unknown value. Simulations were performed for ΔP values of 0.02, 0.03, and 0.04. The first of the 4 simulations presented in Figure 5a corresponds to an oxidation front situated between the depths of 0.1 and 0.3 m, for a simulation oxidation efficiency (quantity of $CH_4$ consumed per unit of time divided by the influx of $CH_4$) of 50%, and ΔP = 0.05 kPa. The other simulations presented (not all are shown) were performed by varying the simulation oxidation efficiency and the position of the oxidation front. As shown in Figure 5a, the best visual reproduction of the observed profile was obtained for a simulation oxidation efficiency of 99%, an oxidation front situated at 0.2 to 0.3 m and ΔP = 0.05 kPa. For this best reproduction, the $CH_4$ influx is 12.2 g $m^{-2}$ $j^{-1}$ (0.017 $m^3$ $m^{-2}$ $j^{-}1$), which corresponds to a biogas flow of 43.1 g $m^{-2}$ $j^{-1}$ (0.033 $m^3$ $m^{-2}$ $j^{-1}$).

**Aug 8, 2006:** As shown in Figure 6, simulations were carried out for several values of ΔP. The best reproduction was obtained for ΔP = 0.03 kPa, associated with a simulation oxidation efficiency of 99% and an oxidation front situated at 0.2 to 0.3 m. The $CH_4$ influx is 4.1 g $m^{-2}$ $j^{-1}$ (0.006 $m^3$ $m^{-2}$ j-1), corresponding to a biogas flow of 14.4 g $m^{-2}$ $j^{-1}$ (0.011 $m^3$ $m^{-2}$ $j^{-1}$), which is approximately 4 times less than the value obtained for August 15, 2006. Slightly higher values of $S_w$ along the profile (89% to 92%) and – especially – a lower ΔP than on August 15, may partially explain this result.

**Sep. 1, 2006:** The results of Figure 7 show that the best reproduction of the field profile is obtained for a simulation oxidation efficiency of 80%, an oxidation front situated between 0.2 to 0.3 m and ΔP = 0.05 kPa. The $CH_4$ influx is 12.6 g $m^{-2}$ $j^{-1}$ (0.018 $m^3$ $m^{-2}$ $j^{-1}$), corresponding to a biogas flow of 36.7 g $m^{-2}$ $j^{-1}$ (0.030 $m^3$ $m^{-2}$ $j^{-1}$), therefore in the same magnitude as that obtained for August 15, 2006. The simulations made it possible to very closely reproduce the $CH_4$ concentration profile in the last 0.3 m, which shows that TOUGH2-LGM is capable of reproducing profiles with very different shapes.

## Simulation of $O_2$ penetration

In order to determine the different depths reached by $O_2$ in the PMOB for different conditions, a series of 9 simulations was performed. This series combined 3 values of degrees of water saturation, i.e. $S_w$ = 75 %, 80 % and 85 %, with 3 pressure differentials between the base and the top of the PMOB, i.e. ΔP = 0.05 kPa, 0.1 kPa and 0.3 kPa.

Figure 8a presents the $CH_4$ concentration profiles when ΔP = 0.05 kPa and when $S_w$ consecutively takes the values of 75%, 80%, and 85%. As expected, the increase in $S_w$ results in a shallower migration of $O_2$. The depths where the "limiting concentration" of 3% of $O_2$ (assuming the value considered by De Visscher et al. (1999) are attained) are the following: 0.28 m (for $S_w$ = 75%), 0.18 m (for $S_w$ = 80%), and 0.09 m (for $S_w$ = 85%). Figure 8b presents the $CH_4$ concentration profiles when ΔP = 0.1 kPa and $S_w$ consecutively takes the same 3 values. The same observations apply as in the case of Figure 8a, but the "limiting concentration" of 3% of $O_2$ is observed closer to the surface.

As discussed earlier, the concept of "limiting concentration" must be considered with care. The fact that $O_2$ concentrations are lower than 3% does not mean that methane oxidation is not taking place. However, according to Gebert et al. (2003), for concentrations lower than 2%, it would not be fully developed. When ΔP = 0.3 kPa (no profiles presented for this case), the $O_2$ concentration is lower than 3% at a depth as shallow as 0.04 m. In this case, the high pressure gradient induces a strong upward advective flux of $CH_4$, which renders the downwards migration of $O_2$ more difficult. As a consequence, it is likely that microbial oxidation will not be very strong within the cover material.

The results of Figure 8a corroborate those reported by Dever et al. (2005), who obtained $O_2$ penetration depths varying between 0 and 0.15 m for a 1.2 m thick biofilter consisting of compost and wood chips. The environmental conditions of the biofilter were in part similar to those used in the simulations, i.e. ΔP was in the order of 0.02 kPa and the biogas arriving at the base of the biofilter had $CH_4$ and $CO_2$ concentrations of 60% and 40% respectively. However, Dever et al.'s (2005) volumetric moisture contents ($\theta_w$) of the biofilter varied between 0% to

25%, which implies higher air porosities ($\theta_a$) than in the St-Nicéphore PMOB site, making it easier for gas to migrate. Also the Dever et al. (2005) biofilter was submitted to temperatures in the vicinity of 40°C, whereas this level of temperature was not attained during the study at St-Nicéphore.

Table 1 presents the $CH_4$ fluxes obtained for the 9 simulations and records the different depths where the 3% $O_2$ concentration threshold was found. It shows that pressure differentials as low as 0.05 kPa can result in a decrease of $O_2$ penetration depth in the order of 0.2 m. This in turn implies a definite decrease in potential bacterial oxidation within a POBM.

The results in Table 1 also show that the $O_2$ penetration depth may also be associated with the ratio between the advective and diffusive fluxes (TOUGH2-LGM makes it possible to discriminate between the two types of transport phenomena). In this way, the analysis of the influence of $S_w$ and $\Delta P$ on $O_2$ penetration can be simplified by only using the single ratio between advection and diffusion. Since the relevant emissions are those reaching the surface, it was decided to take into account the fluxes passing through the element of the model closest to the surface. The highest advective fluxes of $CH_4$ correspond to the highest $\Delta P$ (see equation [1]). Similarly, the diffusive flux of $CH_4$ decreases as $S_w$ increases (see equation [6]).

Figure 9 shows that there is a strong correlation between the depth of $O_2$ penetration and the advection/diffusion ratio. This type of information may be useful in the preliminary stages of selecting which materials to use in a PMOB and for defining placement conditions. Indeed, depending on the choice of materials and on the construction conditions, different structures may be obtained, which affect the values of $K_g$ and $D_s$, thus the depth of $O_2$ penetration, and the potential oxidation efficiency of the PMOB. One can consider the depth where $O_2$ reaches 3% as the required thickness of the oxidation layer (PMOB). Instead of 3%, the value proposed by Gebert et al. (2003) (2% can be used); better yet, a more substrate-specific value should be employed. This value would be obtained from a graphical relationship established between the variation of the oxidation rate and the $O_2$ concentration, such as obtained in the laboratory by Gebert et al. (2003).

Figure 9 also shows the result of the analysis of data from Oct 2, 2006 (Figure 3), for which no oxidation was considered in the simulation. In this particular case, a quite high advection to diffusion ratio was obtained, which explains why the depth of penetration was only 0.02 m.

One has to bear in mind that events, such as a momentary failure of the biogas collection system or a sharp drop in atmospheric pressure, may cause a temporary increase in the advective and diffusive flux ratio and temporarily decrease the performance of the PMOB. Similarly, a succession of rain events would saturate the PMOB, which would increase $S_w$, and therefore reduce $O_2$ penetration. One way to alleviate this problem when designing a POBM is to select a substrate and biogas distribution layer which provides adequate water retention and porosity, so that these materials drain well.

It is also important to consider in the design the potential creation of a hydraulic barrier between the substrate and the gas distribution layer. This breakdown results from a contrast in the hydraulic conductivities of the two materials; when it occurs, the degree of water saturation of

the substrate at the interface between the two materials may become too high and affect biogas migration (Cabral et al. 2007a). For example, it may lead to preferential flow and – in extreme cases - result in the formation of Exopolymeric substances (Hilger et al. 2000).

## Study of the migration and consumption of $O_2$ based on field data

The $[O_2\%]/[N_2\%]$ ratios for the depth of 0.1 m at several sampling dates are presented in Table 2, whereas Table 3 presents the values for the same dates but for a depth of 0.2 m. The values of $N_2$ were back calculated by assuming that the only gases that fill the pores are $O_2$, $CO_2$, $CH_4$ and $N_2$. As a consequence, $[N_2\%] = 100\ \% - ([O_2\%] + [CH_4\%] + [CO_2\%])$.

| $S_w$ (%) | $\Delta P$ (kPa) | Total $CH_4$ flux (g $m^{-2}$ $s^{-1}$) | Diffusive $CH_4$ flux (g $m^{-2}$ $s^{-1}$) | Advective $CH_4$ flux (g $m^{-2}$ $s^{-1}$) | Advection / Diffusion ratio (-) | Depth where [O2]=3% (m) |
|---|---|---|---|---|---|---|
| 75% | 0.05 | 3.6E-04 | 3.3E-04 | 2.7E-05 | 0.08 | 0.275 |
| 80% | 0.05 | 2.9E-04 | 2.6E-04 | 3.2E-05 | 0.12 | 0.175 |
| 85% | 0.05 | 2.2E-04 | 1.8E-04 | 4.1E-05 | 0.23 | 0.09 |
| 75% | 0.1 | 8.1E-04 | 6.9E-04 | 1.2E-04 | 0.18 | 0.125 |
| 80% | 0.1 | 6.5E-04 | 5.1E-04 | 1.4E-04 | 0.27 | 0.08 |
| 85% | 0.1 | 4.9E-04 | 3.3E-04 | 1.6E-04 | 0.50 | 0.05 |
| 75% | 0.3 | 2.6E-03 | 1.7E-03 | 9.3E-04 | 0.55 | 0.04 |
| 80% | 0.3 | 2.1E-03 | 1.1E-03 | 9.6E-04 | 0.85 | 0.03 |
| 85% | 0.3 | 1.6E-03 | 6.1E-04 | 9.7E-04 | 1.57 | 0.025 |

NB: the fluxes indicated are those at the interface between the top-most element and the atmosphere

Table 2 shows that the $[O_2\%]/[N_2\%]$ ratio at 0.1 m was always lower than that between these two gases in the atmospheric air (0.264), which means that there is less $O_2$ than what would normally be found had there been no oxidation. In other words, $O_2$ was consumed – presumably due to the activity of methanotrophs – within the PMOB. Microbiological analysis results of samples collected at Saint Nicéphore in 2006 show, in fact,, a strong presence and activity of methanotrophs on the surface of the PMOB1 (Cabral et al. 2007b; Jugnia et al. 2008). The data from Table 2 also show that $O_2$ is not always present in sufficient quantities (3 % and greater), and that the highest oxidation efficiencies are observed during the days when the $O_2$ concentrations were the highest (see Figure 5 and Figure 6). This observation reinforces the idea that it is $O_2$ availability that limits oxidation.

In the case of field values for the depth of 0.2 m (Table 3), the $[O_2\%]/[N_2\%]$ ratio is always lower than that in the air, with the exception of the last sampling date (Oct 16$^{th}$). This suggests strong microbial activity at this depth (Cabral et al. 2007b) until temperatures start to fall in early October slowing down microbial activity, which steadily brings the $[O_2\%]/[N_2\%]$ ratio back to 0.264. The fact that the $[O_2\%]/[N_2\%]$ ratio on Oct 16$^{th}$ is greater than 0.264 may be associated with the sudden increase in atmospheric pressure (more than 1 kPa in one day). However, it may also be associated with measurement errors coupled with the fact that Table 3 reports average values from 4 profiles in PMOB1.

The results presented in Tables 2 and 3 corroborate those of the numeric simulations with consideration of oxidation performed for the conditions existing at PMOB1 on August 8$^{th}$ and August 15$^{th}$. According to the results obtained, the oxidation efficiencies were approximately 99% and the oxidation front was situated between the depths of 0.2 m and 0.3 m (upper part of the profile).

# Conclusion

The dynamics of methane migration and oxidation by the downward penetration of $O_2$ within a PMOB was studied using the finite element simulator TOUGH2-LGM. Validation of the simulator was performed in two steps; first not considering any oxidation of $CH_4$ and second considering that oxidation occurred.

Inspection of the results shows that TOUGH2-LGM was able to quite accurately reproduce various types of profiles obtained in the field. Also relevant, is TOUGH2-LGM's ability to allow for the evaluation of the oxidation efficiency. The results of the models are sensitive to the gas diffusion coefficient ($D_s$) and the gas permeability ($K_g$) of the substrate, which reinforces the need to properly obtain these parameters for each material to be considered as potential substrate for PMOBs.

The simulator also allowed for the determination of the depth of the oxidation front and to predict the depth of $O_2$ penetration as a function of climatic conditions, namely atmospheric pressure (which affects the pressure differential between the waste mass and the surface) and precipitation (which affects the degree of water saturation within the PMOB). The results have clearly shown that the $O_2$ penetration depth exponentially decreases with an increase in the advection/diffusion ratio. As a result, the design must be done in a way that favors $O_2$ penetration the majority of the time.

One important limitation of TOUGH2-LGM is its inability to simulate both $CH_4$ oxidation and $O_2$ penetration. In fact, this simulator considers $O_2$ and $N_2$ as being a single gas, which would mean that these gases migrate at the same speed within the PMOB and that their concentration ratio is constant along the profile. Although it is possible to use a constant ratio under steady state conditions, this is no longer valid in transient conditions. Since the initial concentration gradients between the surface and the base are different for the two gases and these gradients are modified by oxidation, in addition to the fact that the location of the oxidation front moves with time, the ratio is not constant in a transient state, which is the condition that most closely resembles reality. Therefore, in order for TOUGH2-LGM to become a better prediction tool, it would have to treat $O_2$ and $N_2$ independently and be able to consider the $CH_4$ oxidation reaction.

References


Aachib, M., Mbonimpa, M., and Aubertin, M. 2004. Measurement and prediction of the oxygen diffusion coefficient in unsaturated media, with applications to soil covers. Water, air, and soil pollution, **156**(1): 163-193.

Allaire, S., Lafond, J., and Cabral, A.R. 2007. Measuring gas diffusion in landfill cover material. *In* 11th Intern. Waste Mgmt and Landfill Symp. *Edited by* R. Cossu, R. Stegmann, and T.H. Christensen. Cagliari, Italy. 1-6 Oct., 2007, pp. CD-Rom.

Bear, J., and Bachmat, Y. 1991. Introduction to modeling transport phenomena in porous media. Kluwer Academic Publishers, Dordrecht.

Berger, J., Fornes, L.V., Ott, C., Jager, J., Wawra, B., and Zanke, U. 2005. Methane oxidation in a landfill cover with capillary barrier. Waste Management, **25**(4 SPEC ISS): 369-373.

BNQ 2005. Organic Soil Conditioners - Composts - Certification Protocol (0413-200/2005), Bureau de normalisation du Québec, Québec.

Boeckx, P., and Van Cleemput, O. 2000. Methane oxidation in landfill soils. *In* Trace gas emissions and plants. Kluwer, The Netherlands. pp. 197-213.

Boeckx, P., De Visscher, A., and Van Cleemput, O. 1999. Methane oxidation in landfill cover soil: State of the art. Studiedag 'Stortgas in Vlaanderen', Pellenberg.

Bour, O., Taffoureau, E., and Therrien, R. Lateral landfill gas migration : Characterisation and preliminary modeling results. *In* 9th Intl. Waste Management and Landfill Symposium. 2003, Vol.Santa Margarita di Pula, Sardinia, Italy, p. CD.

Cabral, A.R., Parent, S.-É., and El Ghabi, B. 2007a. Hydraulic aspects of the design of a passive methane oxidation barrier. *In* 2nd BOKU Waste Conf. *Edited by* P. Lechner. Vienna. April 16-19, pp. 223-230.

Cabral, A.R., Arteaga, K., Rannaud, D., Aït-Benichou, S., Pouët, M.F., Allaire, S., Jugnia, L.-B., and Greer, C.W. 2007b. Analysis of methane oxidation and dynamics of methanotrophs within a passive methane oxidation barrier. *In* 11th International Waste Management and Landfill Symposium. Sta. M. di Pula, Italy. 1-6 Oct., Vol.CD-Rom.

Corey, A.T. 1957. Measurement of water and air permeability in unsaturated soil. Soil Science Society of America Proceeding, **1**: 7-10.

Czepiel, P., Mosher, B., Crill, P., and Harriss, R. 1996. Quantifying the effect of oxidation on landfill methane emissions. Journal of Geophysical Research, **101**(11): 16721-16729.

De Visscher, A., Thomas, D., Boeckx, P., and Van Cleemput, O. 1999. Methane oxidation in simulated landfill cover soil environments. Environmental Science and Technology, **33**(1): 1854-1859.

Dever, S.A., Swarbrick, G.E., Annett, L., and Stuetz, R.M. 2005. The effect of landfill gas loading on the performance of a passive biofiltration system operating under australian conditions. *In* Tenth International Waste Management and Landfill Symposium. 2005. CISA, Vol.proceedings CD.

Galle, B., Samuelsson, J., Svensson, B.H., and Borjesson, G. 2001. Measurements of methane emissions from landfills using a Time Correlation Tracer method based on FTIR absorption spectroscopy. Environmental Science and Technology, **35**(1): 21-25.

Gebert, J., and Gröngröft, A. 2006a. Performance of a passively vented field-scale biofilter for the microbial oxidation of landfill methane. Waste Management, **26**(4): 399-407.

Gebert, J., and Gröngröft, A. 2006b. Passive landfill gas emission - Influence of atmospheric pressure and implications for the operation of methane-oxidising biofilters. Waste Management, **26**(3): 245-251.

Gebert, J., Gröngröft, A., and Miehlich, G. 2003. Kinetics of microbial landfill methane oxidation in biofilters. Waste Management, **23**(7): 609-619.

Hettiaratchi, P., and Pokhrel, D. 2003. A New Approach to Quantify Methane Oxidation in a Landfill Bio-Cover: Experience with a Pilot Scale Landfill Test. *In* 9th Int. Waste Mgmt and Landfill Symp. Sta Margarita di Pula, Italy. October 6-10, p. Paper 485.

Hilger, H., and Humer, M. 2003. Biotic Landfill Cover Treatments for Mitigating Methane Emissions. Environmental Monitoring and Assessment, **84**(1): 71-84.

Hilger, H.A., Cranford, D.F., and Barlaz, M.A. 2000. Methane oxidation and microbial exopolymer production in landfill cover soil. Soil Biol. Bioch., **32**: 457-467.

Huber-Humer, M., and Lechner, P. 2002. Proper bio-covers to enhance methane oxidation - findings from a two year field trial. *In* 25th annual Landfill Gas Symposium. Monterey, CA. SWANA (publ. GR-LG-00325), pp. 101-113.

Humer, M., and Lechner, P. 2001a. Microbial Methane Oxidation for the Reduction of Landfill Gas Emissions. Journal of Solid Waste Technology and Management, **Vol. 27**: No. 3-4.

Humer, M., and Lechner, P. 2001b. Microorganisms against the Greenhouse Effect â€“ Suitable Cover Layers for the Elimination of Methane Emissions from Landfills. *In* Proceedings from the Solid Waste Association of North Americaâ€™s (SWANA). Publication GR-LM-0006. 2001. 6th Annual Landfill Symposium, Vol.San Diego, California, pp. 305-318.

IPCC 2001. Climate Change 2001: The Scientific Basis. Contribution of Working Group I to the Third Assessment Report of the Intergovernmental Panel on Climate Change, IPCC, Cambridge.

IPCC 2007. Climate Change 2007 - The Physical Science Basis. *In* Contribution of Working Group I to the Fourth Assessment Report of the IPCC. Cambridge university press, NY.

Jugnia, L.B., Aït-Benichou, S., Fortin, N., Cabral, A.R., and Greer, C.W. 2008. Activity, dynamics and diversity of methanotrophs within an experimental landfill cover Soil Science of America Journal, **(submitted)**.

Jury, W.A., Gardner, W.R., and Gardner, W.H. 1991. Soil Physics, 5th ed. John Wiley & Sons Inc., NY, NY.

Kallistova, A.Y., Kevbrina, M.V., Nekrasova, V.K., Glagolev, M.V., Serebryanaya, M.I., and Nozhevnikova, A.N. 2005. Methane oxidation in landfill cover soil. Microbiology, **74**: 608-614.

Kjeldsen, P. 1996. Landfill gas migration in soil. *In* Landfilling of waste: Biogas. E&FN Spon, London.

Lai, S.H., J.M., T., and A.E., E. 1976. In situ measurement of gas diffusion coefficient in soils. Soil Sci. Soc. Am. J., **40**: 3-6.

Maciel, F.J., and Jucá, J.F.T. 2000. Laboratory and filed tests for studying gas flow through MSW landfill cover soil. *In* Geotechnical Special Publication number 99. *Edited by* C.D. Shackelford, S.L. Houston, and N.-Y. Chang, pp. 569-585.

Millington, R.J., and Quirk, J.P. 1961. Permeability of porous solids. Trans. Faraday Soc., **57**: 1200-1207.

Moldrup, P., Olesen, T., Rolston, D.E., and Yamaguchi, T. 1997. Modeling diffusion and reaction in soils : VII. Predicting gas and ion diffusivity in undisturbed and sieved soils Soil Science, **162**: 632-640.

Morcet, M., Aran, C., Bogner, J., Chanton, J., Spokas, K., and Hebe, I. 2003. Methane mass balance: a review of field results from three french landfill case studies. *In* Ninth International Waste Management and Landfill Symposium. Sta Margarita di Pula, Italy. 2003. CISA, Vol.proceedings CD.

Nagaraj, T.S., Lutenegger, A.J., Pandian, N.S., and Manoj, M. 2006. Rapid estimation of compaction parameters for field control. Geotechnical Testing Journal, **29**(6): 497-506.

Nastev, M. 1998. Modeling Landfill Gas Generation and Migration in Sanitary Landfills and Geological Formations. Ph.D. Thesis, Université Laval, 373.

Nastev, M., Lefebvre, R., Therrien, R., and Gélinas, P. 2003. Numerical modelling of lateral landfill gas migration. Journal of solid waste technology and management, **29**(4): 265-276.

Nolting, B., Gössele, P., Wefer, H., and Bender, M. 1995. Use of water balances for landfill site monitoring. *In* 5th Internationa Landfill Symposium. Sta Margarita di Pula, Italy. 1995, pp. 263-273.

Vigneault, H., Lefebvre, R., and Nastev, M. 2004. Numerical simulation of the radius of influence for landfill gas wells. Vadoze Zone Journal, **3**: 909-916.

Zeiss, C.A. 2006. Accelerated methane oxidation cover systems to reduce greenhouse gas emissions from MSW landfills in cold-semi-arid regions. Water, Air, and Soil Pollution, **176**: 285-306.

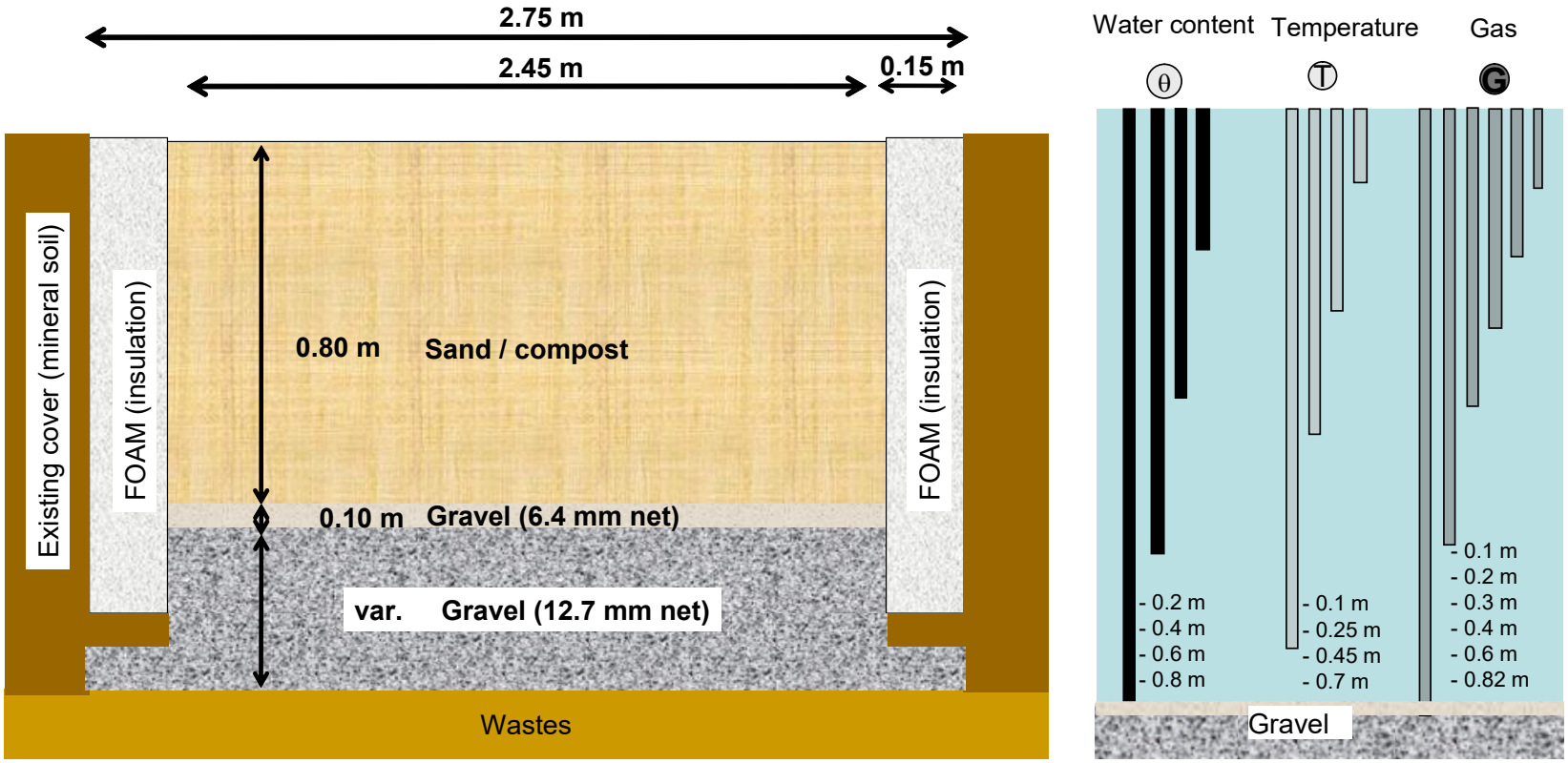


Figure 1 – Schematic Representation of the profile of PMOB1 and Instrument Location

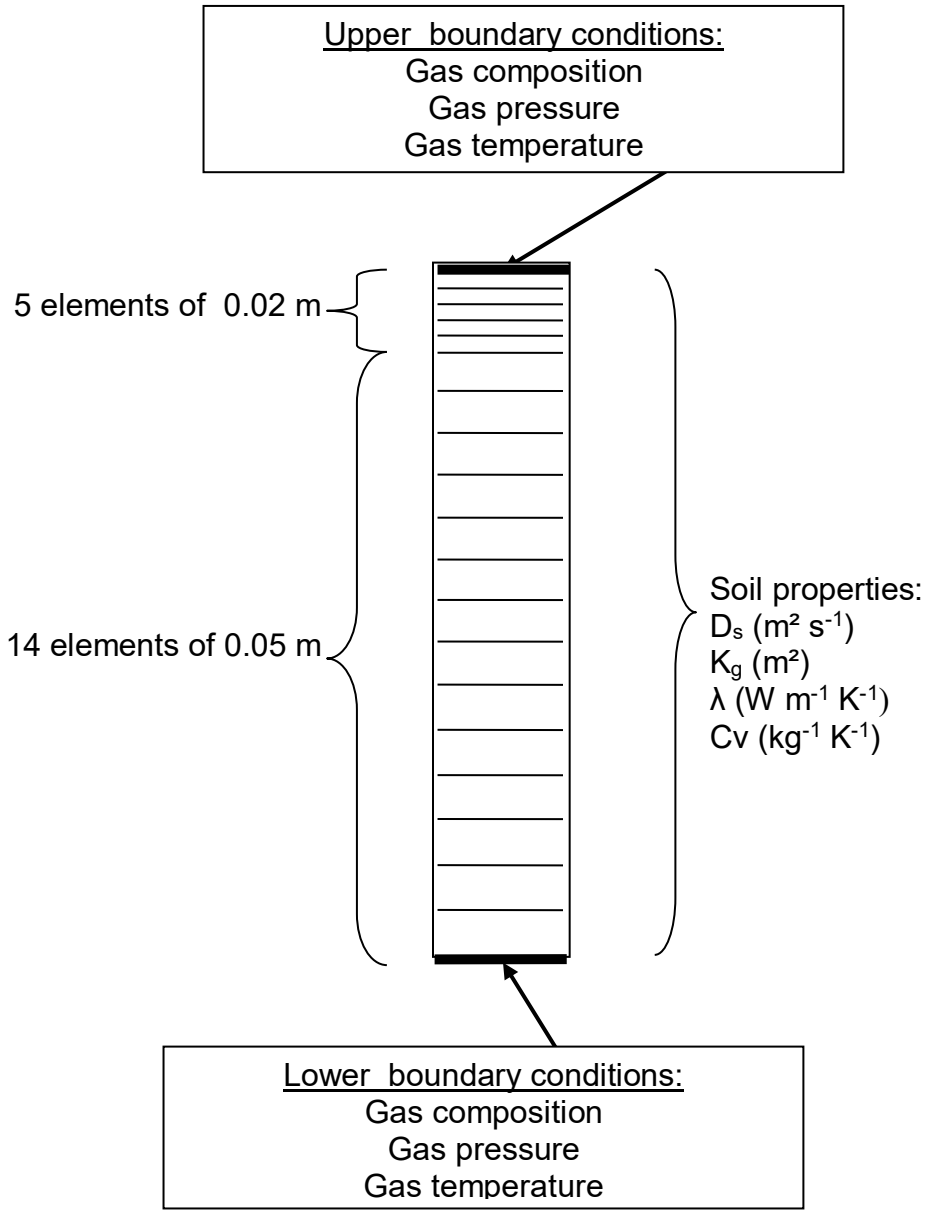


Figure 2 – Schematic Representation of a Typical Simulation using TOUGH2-LGM

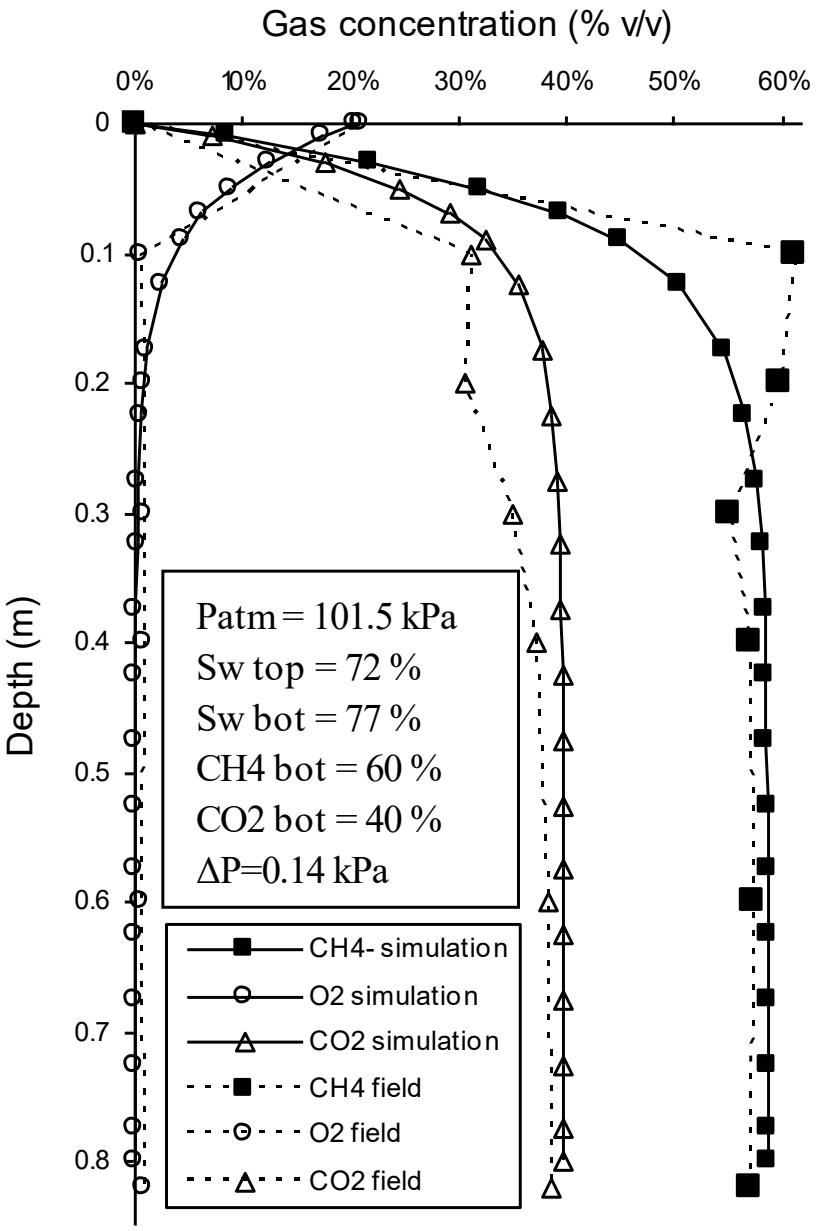


Figure 3 – CH4, CO2, and O2 Average Concentration Profiles for BOPM2 on October 2, 2006 and Profiles Obtained by Simulation with TOUGH2-LGM without Consideration of the Oxidation

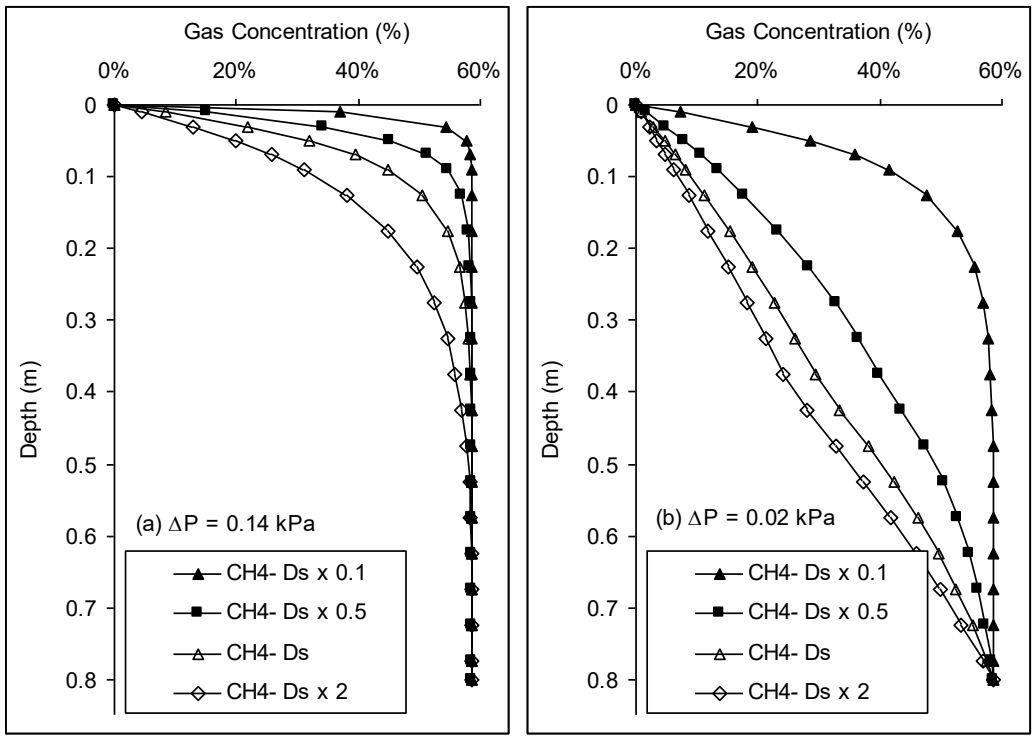


Figure 4 – CH4 Concentration Profiles Obtained by TOUGH2-LGM for Different Values of Ds with (a) ΔP=0.14kPa (Oct. 2, 2006 case; BOPM2); (b) ΔP=0.02kPa

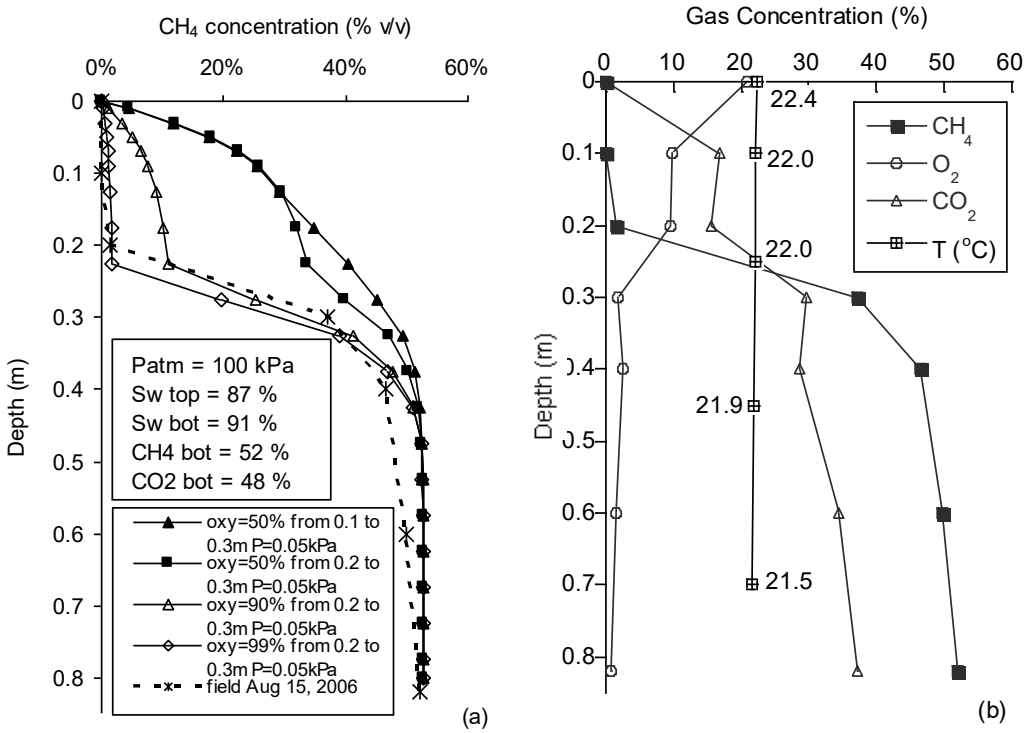


Figure 5 – (a) $CH_4$ Concentration Profiles Obtained by Simulations, as well as in the Field for PMOB1, on August 15, 2006; (b) $CH_4$, $CO_2$, $O_2$ Concentration Profiles and Temperatures Observed in the Field on the Same Date

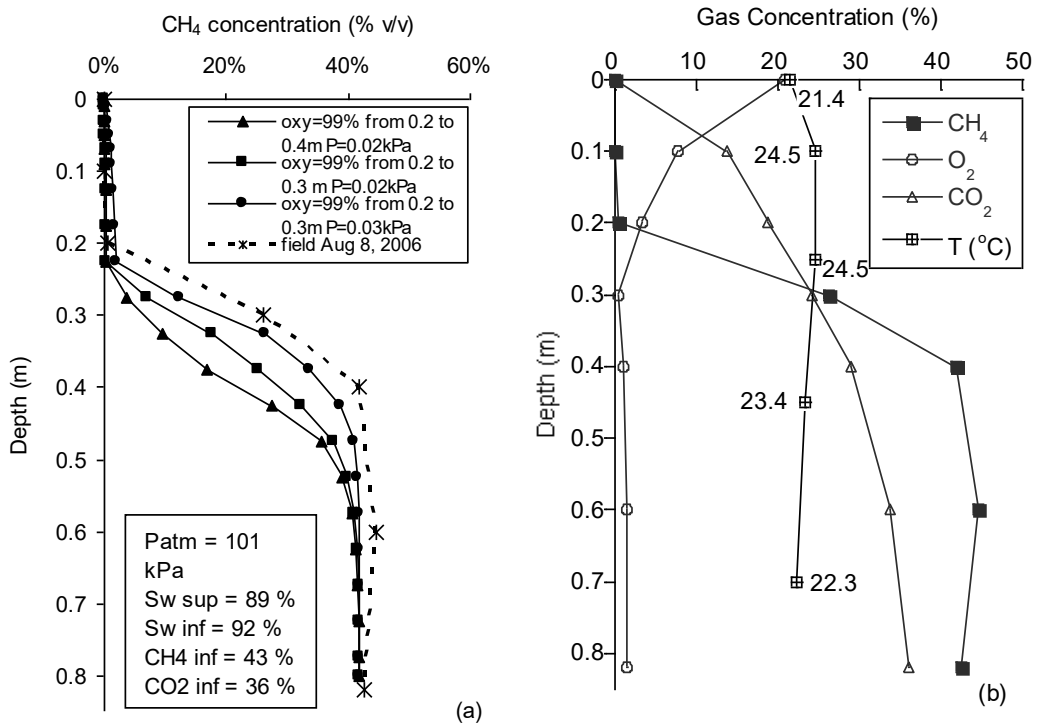


Figure 6 – (a) $CH_4$ Concentration Profiles Obtained in the Field for PMOB1, on August 8, 2006, as well as by Simulations with Consideration of Oxidation; (b) $CH_4$, $CO_2$, and $O_2$ Concentration Profiles Observed in the Field on the Same Date

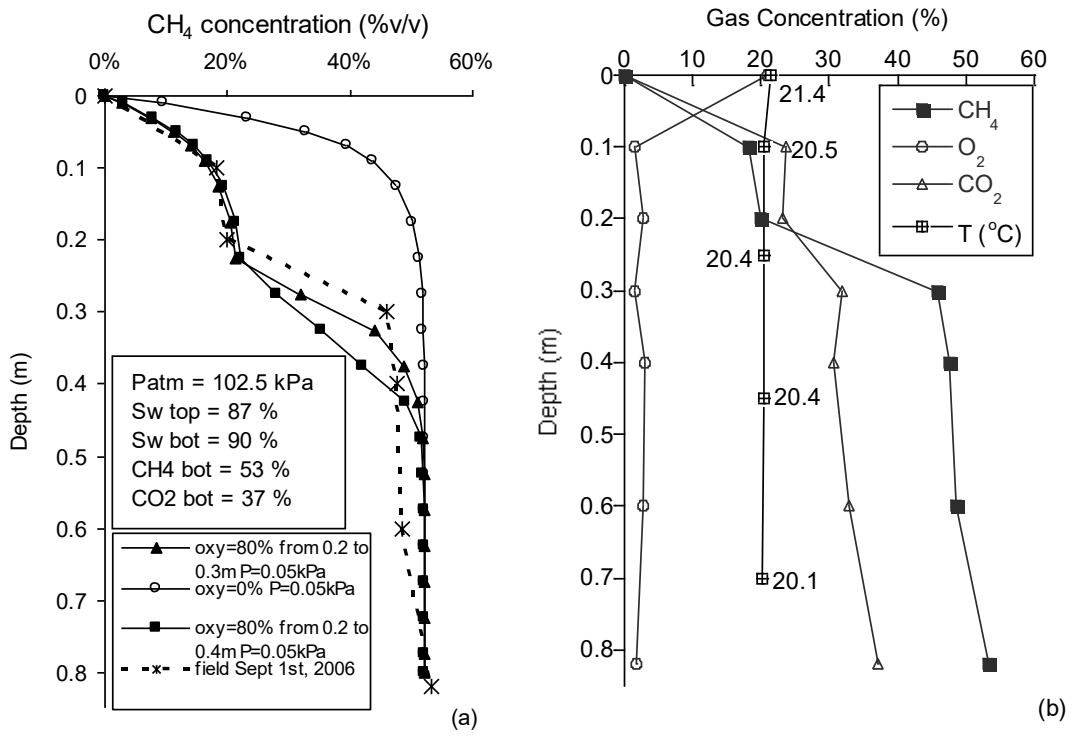


Figure 7 – (a) $CH_4$ Concentration Profiles Obtained in the Field (BOPM1), on Sep 1, 2006, as well as by Simulations with Consideration of Oxidation; (b) $CH_4$, $CO_2$, and $O_2$ Concentration Profiles Observed in the Field on the Same Date

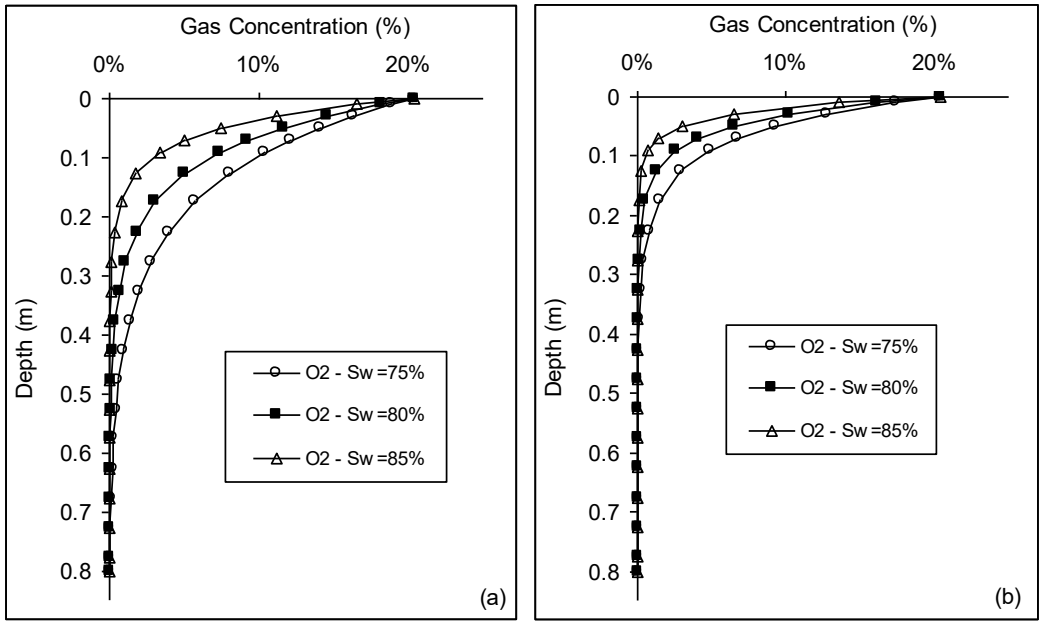


Figure 8 - $O_2$ Concentration Profiles with (a) $\Delta P = 0.05$ kPa; (b) $\Delta P = 0.1$ kPa

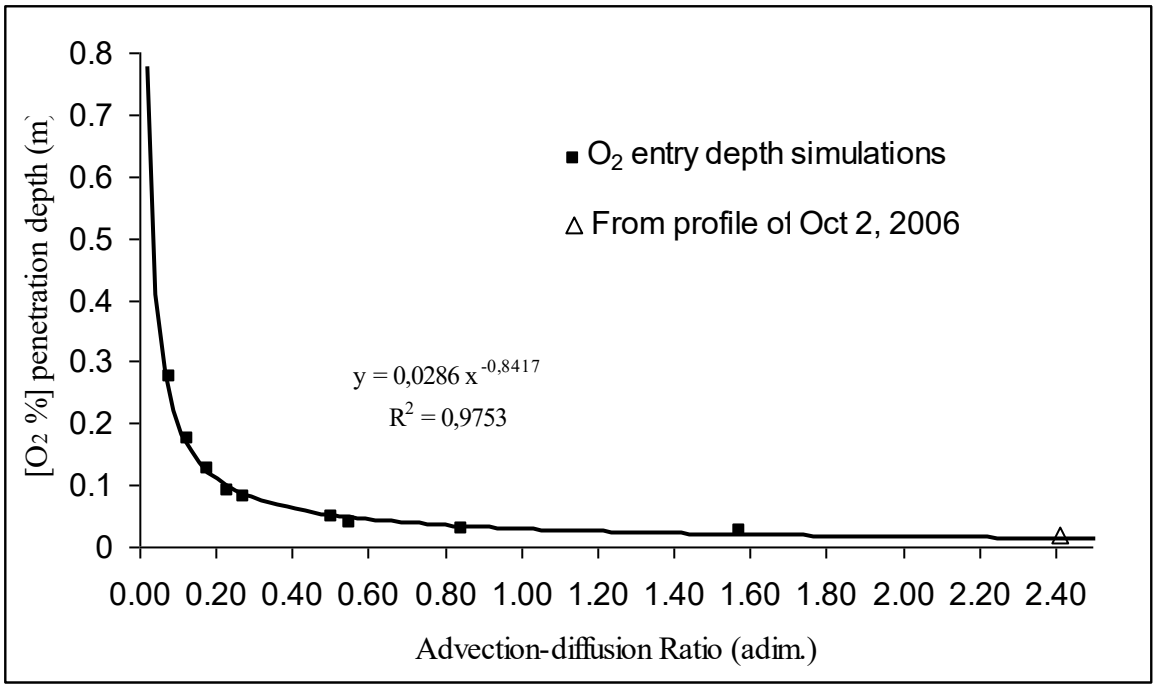


Figure 9 - [$O_2$ %] Penetration Depth as a Function of the Advection/Diffusion Ratio

Table 1 - Results of 9 simulations using TOUGH2-LGM

| $S_w$ (%) | $\Delta P$ (kPa) | Total $CH_4$ flux (g $m^{-2}$ $s^{-1}$) | Diffusive $CH_4$ flux (g $m^{-2}$ $s^{-1}$) | Advective $CH_4$ flux (g $m^{-2}$ $s^{-1}$) | Advection / Diffusion ratio (-) | Depth where [O2]=3% (m) |
|---|---|---|---|---|---|---|
| 75% | 0.05 | 3.6E-04 | 3.3E-04 | 2.7E-05 | 0.08 | 0.275 |
| 80% | 0.05 | 2.9E-04 | 2.6E-04 | 3.2E-05 | 0.12 | 0.175 |
| 85% | 0.05 | 2.2E-04 | 1.8E-04 | 4.1E-05 | 0.23 | 0.09 |
| 75% | 0.1 | 8.1E-04 | 6.9E-04 | 1.2E-04 | 0.18 | 0.125 |
| 80% | 0.1 | 6.5E-04 | 5.1E-04 | 1.4E-04 | 0.27 | 0.08 |
| 85% | 0.1 | 4.9E-04 | 3.3E-04 | 1.6E-04 | 0.50 | 0.05 |
| 75% | 0.3 | 2.6E-03 | 1.7E-03 | 9.3E-04 | 0.55 | 0.04 |
| 80% | 0.3 | 2.1E-03 | 1.1E-03 | 9.6E-04 | 0.85 | 0.03 |
| 85% | 0.3 | 1.6E-03 | 6.1E-04 | 9.7E-04 | 1.57 | 0.025 |

NB: the fluxes indicated are those at the interface between the top-most element and the atmosphere

Table 2 - Average Gas Concentration Values in PMOB1 and $[O_2\%]/[N_2\%]$ Ratio Values at a Depth of 0.1 m

| PMOB 1 - 0.1 m | | | | | |
|---|---|---|---|---|---|
| | Measured | | | Calculated | |
| Date | $CH_4$ (%) | $CO_2$ (%) | $O_2$ (%) | $N_2$ (%) | $[O_2]/[N_2]$ |
| Jul. 20 | 0.01 | 20.55 | 3.75 | 75.69 | 0.05 |
| Aug. 02 | 10.25 | 14.70 | 0.75 | 74.30 | 0.01 |
| Aug. 08 | 0.01 | 13.85 | 7.70 | 78.44 | 0.10 |
| Aug. 15 | 0.01 | 16.88 | 9.68 | 73.44 | 0.13 |
| Sep. 01 | 18.20 | 23.55 | 1.53 | 56.73 | 0.03 |
| Sep. 05 | 53.48 | 35.53 | 1.05 | 9.95 | 0.11 |
| Sep. 11 | 34.23 | 25.93 | 1.83 | 38.03 | 0.05 |
| Sep. 18 | 47.58 | 35.23 | 1.53 | 15.68 | 0.10 |
| Sep. 25 | 55.48 | 34.68 | 0.65 | 9.20 | 0.07 |
| Oct. 02 | 48.75 | 33.75 | 1.75 | 15.75 | 0.11 |
| Oct. 09 | 51.35 | 35.65 | 1.78 | 11.23 | 0.16 |
| Oct. 16 | 52.48 | 34.58 | 1.98 | 10.98 | 0.18 |

Table 3 - Average Gas Concentration Values in PMOB1 and $[O_2\%]/[N_2\%]$ Ratio Values at a Depth of 0.2 m

| PMOB 1 - 0.2 m | | | | | |
|---|---|---|---|---|---|
| | Measured | | | Calculated | |
| Date | $CH_4$ (%) | $CO_2$ (%) | $O_2$ (%) | $N_2$ (%) | $[O_2]/[N_2]$ |
| Jul. 20 | 0.03 | 19.80 | 2.15 | 78.02 | 0.03 |
| Aug. 02 | 12.50 | 14.80 | 2.55 | 70.15 | 0.04 |
| Aug. 08 | 0.51 | 18.80 | 3.35 | 77.34 | 0.04 |
| Aug. 15 | 1.46 | 15.60 | 9.53 | 73.41 | 0.13 |
| Sep. 01 | 20.00 | 23.13 | 2.80 | 54.08 | 0.05 |
| Sep. 05 | 49.58 | 32.70 | 2.38 | 15.35 | 0.15 |
| Sep. 11 | 38.33 | 27.78 | 1.70 | 32.20 | 0.05 |
| Sep. 18 | 49.85 | 36.43 | 0.98 | 12.75 | 0.08 |
| Sep. 25 | 55.10 | 35.40 | 0.83 | 8.68 | 0.10 |
| Oct. 02 | 51.60 | 34.68 | 1.55 | 12.18 | 0.13 |
| Oct. 09 | 44.68 | 30.70 | 4.43 | 20.20 | 0.22 |
| Oct. 16 | 49.60 | 32.15 | 4.28 | 13.98 | 0.31 |